& Sarma, M. H., Eds.) pp 287-306, Adenine Press, New York.
Leontis, N. B., Ghosh, P., & Moore, P. B. (1986a) *Biochemistry 25*, 3916-3925.
Leontis, N. B., Ghosh, P., & Moore, P. B. (1986b) *Biochemistry 25*, 7386-7392.
Li, S.-J., & Marshall, A. G. (1985) *Biochemistry 24*, 4047-4052.
Li, S.-J., & Marshall, A. G. (1986) *Biochemistry 25*, 3673-3682.
Li, S.-J., Wu, J., & Marshall, A. G. (1987) *Biochemistry 26*, 1578-1585.
Luehrsen, K. R., & Fox, G. E. (1981) *Proc. Natl. Acad. Sci. U.S.A. 78*, 2150-2154.
Marion, D., & Wüthrich, K. (1983) *Biochem. Biophys. Res. Commun. 113*, 967-974.
Marshall, A. G., & Wu, J. (1990) *Biol. Magn. Reson. 9*, 55-118.
McConnell, B. (1984) *J. Biomol. Struct. Dyn. 1*, 1407-1421.
Muller, J. J., Misselwitz, R., Zirwer, D., Damaschun, G., & Welfle, H. (1985) *Eur. J. Biochem. 148*, 89-95.
Nishikawa, K., & Takemura, S. (1974) *J. Biochem. (Tokyo) 76*, 935-947.
Noller, H. F., & Garrett, R. A. (1979) *J. Mol. Biol. 132*, 621-636.
Patel, D. J. (1977) *Biopolymers 16*, 1635-1656.
Rabin, D., Kao, T. H., & Crothers, D. M. (1983) *J. Biol. Chem. 258*, 10813-10816.
Redfield, A. G., & Kunz, S. D. (1975) *J. Magn. Reson. 19*, 250-254.
Richard, E. G., Lecanidou, R., & Geroch, M. E. (1973) *Eur. J. Biochem. 34*, 262-267.
Robillard, G. T., & Reid, B. R. (1979) in *Biological Applications of Magnetic Resonances* (Shulman, R. G., Ed.) pp 45-112, Academic Press, New York.
Roy, S., Papastavros, M. Z., & Redfield, A. G. (1982) *Biochemistry 21*, 6081-6088.
Sanchez, V., Redfield, A. G., Johnston, P. D., & Tropp, J. (1980) *Proc. Natl. Acad. Sci. U.S.A. 77*, 5659-5662.
Weidner, H., & Crothers, D. M. (1977) *Nucleic Acids Res. 4*, 3401-3414.
Weidner, H., Yuan, R., & Crothers, D. M. (1977) *Nature (London) 266*, 193-194.
Wolters, J., & Erdmann, V. A. (1988) *Nucleic Acids Res. 16*, r1-r45.
Wu, J., & Marshall, A. G. (1990) *Biochemistry* (following paper in this issue).
Wüthrich, K. (1986) *NMR of Proteins and Nucleic Acids*, Wiley, New York.

Wheat Germ 5S Ribosomal RNA Common Arm Fragment Conformations Observed by ^1H and ^{31}P Nuclear Magnetic Resonance Spectroscopy†

Jiejun Wu‡ and Alan G. Marshall*,‡,§
Department of Biochemistry, 484 West 12th Avenue, and Department of Chemistry, 120 West 18th Avenue, The Ohio State University, Columbus, Ohio 43210
Received July 31, 1989

ABSTRACT: The *nonexchangeable* protons of the common arm fragment of wheat germ (*Triticum aestivum*) ribosomal 5S RNA have been observed by means of high-resolution 500-MHz ^1H NMR spectroscopy in D_2O solution. Although NMR studies on the *exchangeable* protons support the presence of two distinct solution structures of the common arm fragment (and of the same base-paired segment in intact 5S rRNA), only a single conformation is manifested in the ^1H NMR behavior of all of the H6 and H5 pyrimidine and most of the H8/H2 purine protons under the same salt conditions. The nonexchangeable protons near the base-paired helix have been assigned by a sequential strategy. Conformational features such as the presence of a cytidine–uridine (C·U) pair at the loop–helix junction and base stacking into the hairpin loop are evaluated from nuclear Overhauser enhancement spectroscopy (NOESY) data. Double-quantum filtered correlation spectroscopy (DQF-COSY) experiments show that most of the 26 riboses are in the C3′-endo conformation. Finally, backbone conformational changes induced by Mg^{2+} and heating have been monitored by ^{31}P NMR spectroscopy. Our results show that the common arm RNA segment can assume two conformations which produce distinguishably different NMR environments at the base-pair hydrogen-bond imino protons but not at nonexchangeable base or ribose proton or backbone phosphate sites.

Recent developments in NMR methodology (in conjunction with large-scale synthesis of oligonucleotides of defined sequences) have produced much recent progress in knowledge in nucleic acid solution structure and dynamics [for reviews, see Gronenborn and Clore (1985), Patel et al. (1987), Hosur et al. (1988), and Van de Ven & Hilbers (1988)]. For example, general resonance assignment procedures have been applied for double-stranded synthetic RNA oligomers which generally form A-type helices. Detailed structural information for smaller oligomers (say, <10000 Da) may be obtained from analysis of ^1H–^1H and/or ^1H–^{31}P coupling constants, ^1H–^1H dipolar cross-relaxation data, extensive computer modeling, or a combination of the above (Clore et al., 1985; Lankhorst et al., 1985; Happ et al., 1988; Van den Hoogen et al., 1988; Chou et al., 1989).

For nucleic acids of larger size (>10000 Da), NMR studies are usually limited to the downfield exchangeable proton region (9–15 ppm from DSS) or to nuclei other than protons (^{31}P, ^{13}C, ^{15}N), due to extensive ^1H NMR peak overlap. For ex-

† This work was supported by grants (to A.G.M.) from the U.S. Public Health Service (NIH 1 R01 GM-29274; NIH 1 S10 RR-01458) and The Ohio State University.
‡ Department of Biochemistry.
§ Department of Chemistry.

0006-2960/90/0429-1730$02.50/0

ample, groups at The Ohio State University and Yale University have studied 5S ribosomal RNAs and their enzymatically cleaved fragments from a variety of organisms by various spectroscopic techniques, especially high-field (11.75 T, 500 MHz for protons) ^{1}H NMR [see review by Marshall and Wu (1990)]. Specifically, the base pairs in the 5S rRNA "common arm" fragment purified from wheat germ (*Triticum aestivum*), corresponding to residues 26–51 in the primary sequence, have been identified (e.g., A·U, G·C) and sequenced (Li et al., 1987; Wu & Marshall, 1990). Several additional resonances (beyond those predicted from the standard Luehrsen–Fox secondary structural model) were detected in the slow-exchangeable proton region (9–15 ppm chemical shift). This anomaly has recently been explained as due to two NMR-distinguishable solution conformations of the molecule (Wu & Marshall, 1990); all imino protons and some amino protons in the base-paired segment could then be assigned for each of the two conformers. Moreover, a C·U base pair was posited from large observed nuclear Overhauser enhancements (NOEs). The helix–loop junction was shown to be quite tightly packed.

In this paper, we extend the investigation of the solution structure of wheat germ 5S rRNA common arm fragment (hereafter called the B2 fragment) to nonexchangeable protons to determine the extent to which conformational differences clearly detected at the base-pair hydrogen-bond protons propagate outward to the bases, sugars, and phosphates. Somewhat surprisingly, we shall show that only one conformation can be detected for each H6 and H5 pyrimidine, as well as for most of the H8 and/or H2 purine protons. Resonance assignments near the helix have been achieved by means of a series of one- and two-dimensional (1-D and 2-D) ^{1}H NMR experiments in D_2O. Sequence-specific conformational feactures are observable, especially in the vicinity of the loop–helix junction. Ribose conformations have been probed by double-quantum filtered correlation spectroscopy (DQF-COSY). In conjunction with data obtained from H_2O solution, we propose that the two conformers differ in the tightness (compactness) of their base-paired helical segments. Finally, structural changes induced in the phosphodiester linkage by heat and Mg^{2+} have been monitored by ^{31}P NMR.

Materials and Methods

NMR Samples. Preparation of wheat germ 5S rRNA and its common arm fragment NMR samples was as previously described (Wu & Marshall, 1990), with the following changes: after being washed with 75% ethanol, the RNA fragments were dissolved in 0.35 mL of 10 mM sodium phosphate, pH 7.0, and lyophilized. The RNA was further lyophilized twice in 99.8% D_2O and finally dissolved in 0.35 mL of 99.996% D_2O. Then the NMR tube was sealed by fire.

Proton NMR Spectroscopy. All proton NMR spectra were obtained with a Bruker AM-500 Fourier transform NMR spectrometer. All spectra were recorded at 297 K unless otherwise specified. Chemical shifts are reported in parts per million relative to 2,2-dimethyl-2-silapentane-5-sulfonate (DSS) as zero, on the basis of an independent calibration. All spectra were subjected to a Lorentz-to-Gauss apodization before Fourier transformation (FT), and no base-line correction was performed except for integration measurements (which were preceded by a fully automatic linear base-line correction—see below).

For the purpose of peak integration, a conventional 1-D ^{1}H NMR spectrum was produced (spectral width of 3759 Hz and 16K time-domain quadrature data, to yield an FT digital spectral resolution of 0.459 Hz/point). The cycle time for each event sequence was 32 s, during which time the residual HDO resonance was presaturated at a decoupler power of 35 dB below 0.2 mW for 4 s.

All 2-D NMR spectra were recorded in phase-sensitive mode, with pure absorption line shape obtained by use of the time-proportional phase incrementation (TPPI) method (Redfield & Kunz, 1975; Marion & Wüthrich, 1983), with a relaxation delay of 3 s. A 3-ms homospoil pulse (HSP) was used after each acquisition to destroy any residual transverse magnetization. The HDO resonance was suppressed by gated homonuclear irradiation in the preparation period (and also during the mixing time in NOESY). The decoupler power was 35 dB below 0.2 mW. A total of 4K time-domain data were acquired in the t_2 dimension (with varying number of t_1 increments—see below). Data in both dimensions were apodized by Lorentz-to-Gauss transformation, and zero filled to 2K in the t_1 dimension before FT. The final digital resolution was 1.84 Hz/point in F_2 and 3.67 Hz/point in F_1 dimensions.

^{1}H–^{1}H homonuclear correlation spectroscopy (COSY) was performed by use of the (HSP–delay–90°–t_1–90°–acquire)$_n$ pulse sequence, with 256 words in the t_1 dimension and 40 scans taken for each t_1 value.

DQF-COSY experiments were performed with the pulse sequence (HSP–delay–90°–t_1–90°–90°–acquire)$_n$. A 3-μs delay was inserted between the last two 90° pulses to allow for proper radio frequency phase switching. A total of 512 t_1 values were used, with 128 acquisitions for each t_1 value.

NOESY experiments were performed with the pulse sequence (HSP–delay–90°–t_1–90°–t_m–90°–acquire)$_n$. The HDO resonance was irradiated during both the relaxation delay (3.6 s) and mixing (0.8 or 0.4 s) periods, at a decoupler power 36 dB below 0.2 mW. Relaxation delay was 3.6 s. Data for 512 t_1 values were acquired, with 64 scans for each t_1 value.

Phosphorus NMR Spectroscopy. All ^{31}P NMR spectra were acquired with a Bruker MSL-300 FT/NMR spectrometer (121 MHz for ^{31}P), equipped for variable-temperature operation. Broadband proton decoupling was achieved by asynchronous F2 irradiation using a WALTZ pulse sequence (3$\underline{4}$2 3$\underline{1}$2 4$\underline{2}$3 3$\underline{4}$2 3$\underline{1}$2 4$\underline{2}$3). The 90° proton pulse (the "1" pulse) was 100 μs. The spectral width was 3649 Hz, with 8K time-domain quadrature data acquired. The time-domain data set was zero filled to 16K before FT. Chemical shifts were referenced to the inorganic phosphate resonance (which is a buffer component) at 297 K. For Mg^{2+} titration, 1-μL increments of 1 M $MgCl_2$ solution were added to the NMR sample tube, and a relaxation delay of 2 ms was used.

Results and Discussion

Identification of Pyrimidine H6 and H5 Resonances from COSY Experiments. A 500-MHz ^{1}H NMR spectrum of the wheat germ 5S rRNA B2 fragment in D_2O solution is shown in Figure 1. In that spectrum, proton types are associated with chemical shift ranges: base protons H2 (of A), H8 (of A or G), H6 (of C or U), 7–8.5 ppm; base protons H5 (of C or U), ribose protons H1′, 5–6.5 ppm; and other ribose protons, 3.5–5 ppm. The base proton and H1′ resonances are relatively well resolved, whereas other ribose proton resonances overlap extensively.

As mentioned above, two B2 fragment conformers in H_2O solution are evident from the appearance of two sets of imino/amino resonances (Wu & Marshall, 1990). Thus, it is natural to expect that *non*exchangeable protons of the two conformers should also exhibit chemical shift differences. Our analysis therefore begins by counting and identifying the number of resonances corresponding to each base or ribose proton type.

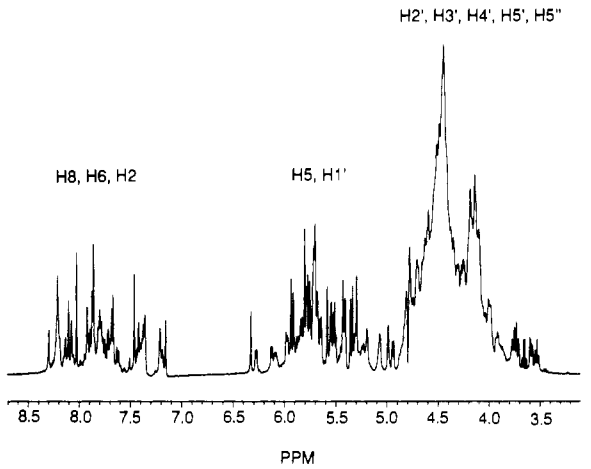

FIGURE 1: 500-MHz ^{1}H NMR spectrum of the wheat germ 5S rRNA common arm fragment in 10 mM sodium phosphate, pH 7.0, 99.996% D_2O solution. The characteristic chemical shifts for various proton types are indicated.

Table I: Chemical Shifts (ppm) of All H6 and H5 and Some H1′ and H2′ Resonances of the Wheat Germ 5S rRNA Common Arm Fragment

H6[a]	H5[a]	H1′[b]	H2′[b]
8.210	6.063	6.108	4.762
8.200	5.686	5.965	4.702
8.180	6.260	5.672	4.652
7.858	5.858	5.405	4.810
7.817	5.812	5.270	4.240
7.785	5.700		
7.756	5.672		
7.728	5.663		
7.691	5.730		
7.663	5.781		
7.387	5.286		
7.366	4.923		
7.358	5.200		

[a] Determined from H6–H5 pairs in Figure 2. [b] Determined from H1′–H2′ pairs in Figure 4.

The pyrimidine (C and U) H6 and H5 proton resonances are well separated and scalar coupled to each other (with homonuclear J coupling constants of about 7 Hz). Thus, they are readily identified by means of COSY experiments. Figure 2 shows part of a phase-sensitive COSY spectrum of the B2 fragment. Thirteen H6–H5 cross peaks appear as typical doublets (also see Table I), in exact correspondence with the 13 pyrimidines in the B2 primary nucleotide sequence, thereby establishing two conclusions. First, the sample is free of observable oligonucleotide contamination. Thus, the observation (Wu & Marshall, 1990) of more imino/amino proton resonances than expected from the standard secondary structure model in H_2O solution is not due to impurities. Second, there is only one NMR-distinguishable conformation for each H6 and H5 in both conformers. This second (unexpected) conclusion may be rationalized in two ways: (a) H6 and H5 protons are located relatively exterior to the inside of the RNA A-helix, where two distinct imino/amino proton environments are seen; (b) the base-paired imino proton and one of the amino protons [NH2(a)] are hydrogen bonded, and their chemical shifts are highly sensitive to the strength of the hydrogen bond. Thus, the two conformers most likely differ in the degree of the hydrogen bonding in the helix region: i.e., one conformer can be regarded as having a more "open" helix (with the *same* base-pair *sequence*) than the other (Wu & Marshall, 1990).

Conformation Differences at H8 and *H2 Based on Spectral Integration.* We now proceed to ask whether any of the other assignable nonexchangeable protons are distinguishable in the two conformations. Figure 3 shows chemical shift expanded spectral segments for the H8/H6/H2 and H5/H1′ resonances, with more pronounced resolution enhancement than that shown in Figure 1. The H8/H6/H2 data are the most informative. If the well-resolved H1′ singlet at 6.312 ppm is taken as having unit area, a total of 35 resonances in the 8.339–7.113 ppm chemical shift range is obtained by spectral integration, in good agreement (if relative peak areas are ignored) with the value of 34 predicted for a single NMR-detectable conformation.

However, if H6 doublets are excluded in the integration process, eight of the remaining resonances (labeled with dots in Figure 3) each appear with relative area of ~0.5. Moreover, at least 27 distinct resonances can be seen in this region, i.e., more than the 21 (excluding H6 doublets) expected if each of the H8 and H2 protons exhibited just a single chemical shift. Thus, it is clear that at least four H8 and/or H2 protons are reporting two NMR-distinguishable conformations. Because H8 and H2 resonances cannot be distinguished at this stage, we cannot say whether the two conformations are manifested at H8 or H2 sites. Finally, no firm conclusions can be drawn from the H5 and ribose proton resonances, because their total integrated intensity is larger than expected for their known

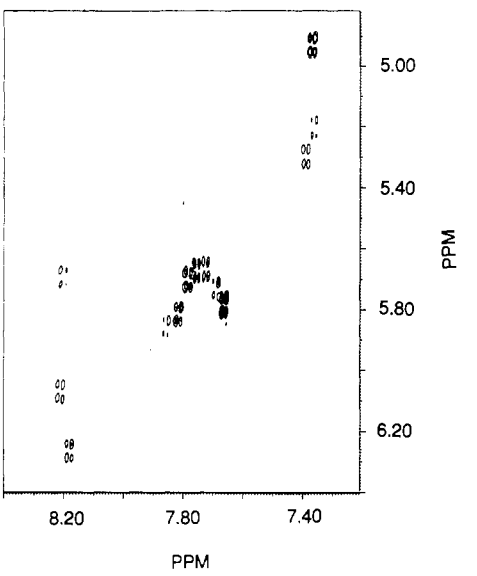

FIGURE 2: Portion of a phase-sensitive 500-MHz ^{1}H–^{1}H homonuclear COSY spectrum of the wheat germ 5S rRNA common arm fragment. Note the presence of 13 H6–H5 cross peaks (see text).

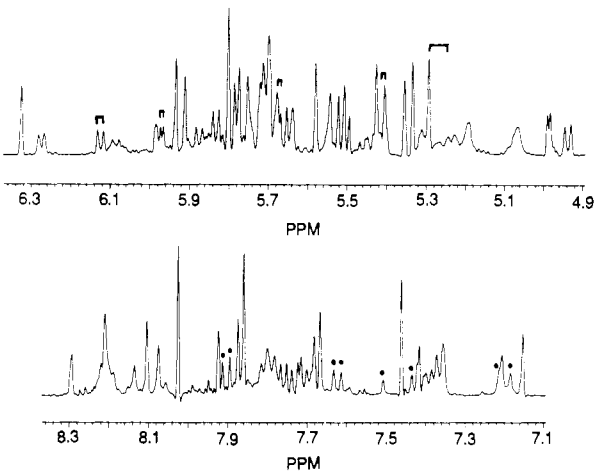

FIGURE 3: Two expanded-scale segments of the spectrum of Figure 1, with more pronounced resolution enhancement. (Top) Base H5 and ribose H1′ protons. Resonances with a bar on top are H1′ doublets. (Bottom) Base H8, H6, and H2 protons. Resonances with a dot on top have half-unit area (see text).

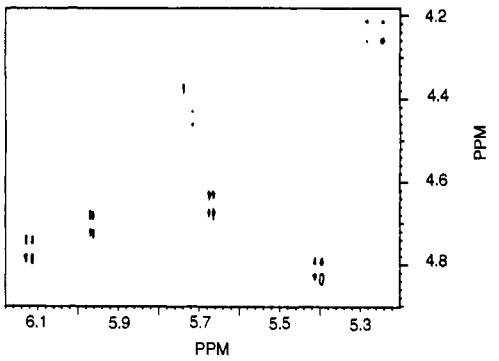

FIGURE 4: Portion of a phase-sensitive 500-MHz ^1H–^1H homonuclear DQF-COSY spectrum of the wheat germ 5S rRNA common arm fragment showing the ribose H1′–H2′ correlation. Five cross peaks are observed (see text).

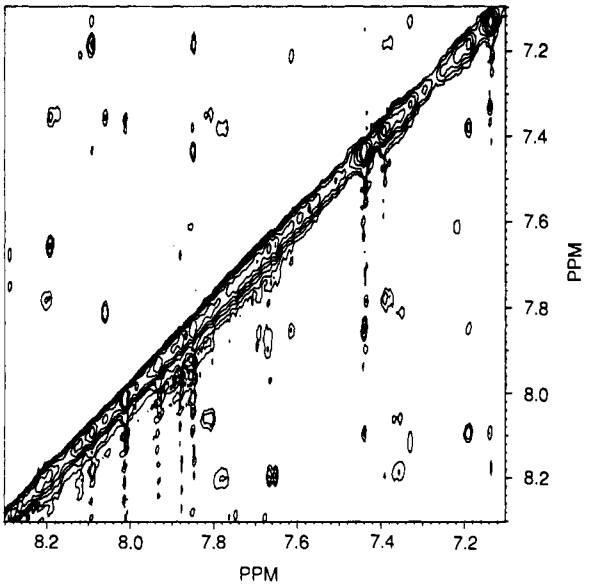

FIGURE 5: Portion of a phase-sensitive 500-MHz ^1H–^1H homonuclear NOESY spectrum (0.8-s mixing time) of the wheat germ 5S rRNA common arm fragment. The $(H8/H6)_n$–$(H8/H6)_{n+1}$ pathway is shown.

number in the molecule. The "extra" spectral intensity in this chemical shift range may result from small-molecule contaminants, which are more likely to show up in the upfield than in the downfield aromatic spectral range.

Sugar Pucker Determined from DQF-COSY Experiments. It is well-known that three-bond ^1H–^1H scalar coupling constants are very sensitive to sugar geometry. The ribose ring in an RNA molecule can adopt several conformations, normally C3′-endo for an A-helix or C2′-endo to accommodate a sharp turn or extension between two residues (Jack et al., 1976). The two types of sugar pucker can be differentiated qualitatively according to the magnitude of the H1′–H2′ J coupling constant, which is small for C3′-endo and large for C2′-endo conformation. Thus, in a COSY-type experiment performed at relatively low resolution, the H1′–H2′ cross peaks will be absent for C3′-endo sugar pucker, owing to the antiphase nature of the cross peak components. A better experiment is double-quantum filtered (DQF) COSY, in which both diagonal and off-diagonal peaks are in antiphase absorption mode, and thus the H1′–H2′ cross peaks can easily be observed. (Normal two-pulse COSY, although more sensitive, has diagonal peaks in double-dispersion mode, which makes the observation of H1′–H2′ cross peaks very difficult.)

Figure 4 shows part of a DQF-COSY spectrum of the B2 fragment, in which only five prominent cross peaks can be seen

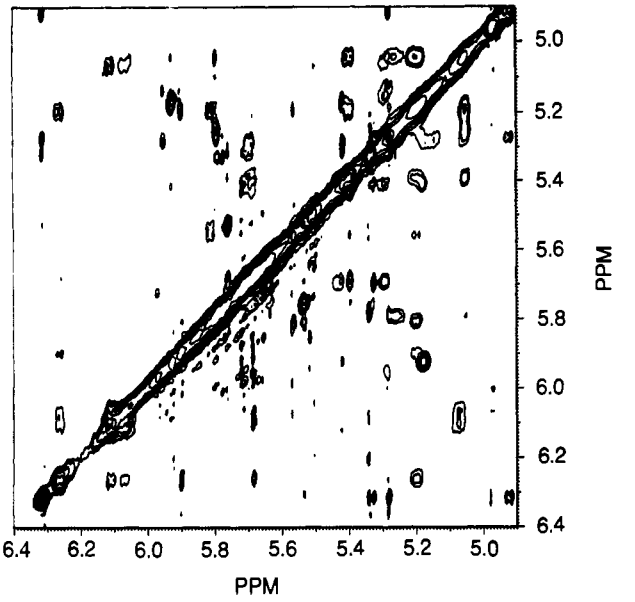

FIGURE 6: Portion of a phase-sensitive 500-MHz ^1H–^1H homonuclear NOESY spectrum (0.8-s mixing time) of the wheat germ 5S rRNA common arm fragment, showing the $(H5/H1')_n$–$(H5/H1')_{n+1}$ pathway.

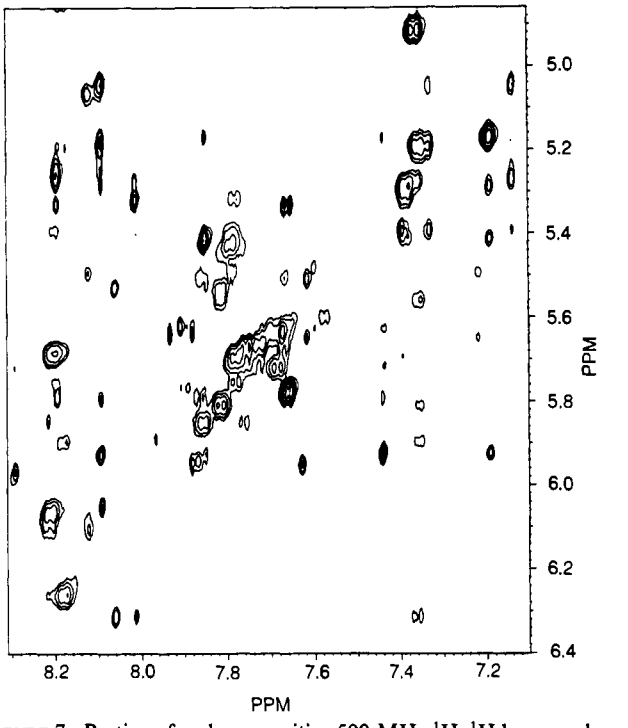

FIGURE 7: Portion of a phase-sensitive 500-MHz ^1H–^1H homonuclear NOESY spectrum (0.4-s mixing time) of the wheat germ 5S rRNA common arm fragment showing the $(H8/H6)_n$–$(H1')_n$–$(H8/H6)_{n+1}$–$(H1')_{n+1}$ pathway.

(also see Table I). Thus, most of the 26 riboses in the primary sequence are in the C3′-endo conformation. The H1′ doublet at 6.108 ppm can be assigned (see below) to residue C_{44}, which participates in the C·U pair at the loop–helix junction; we shall return to discuss that point.

Sequence Assignment of Resonances in or near the Helical Segment. Further characterization of the three-dimensional structure of the B2 fragment was attempted by means of phase-sensitive NOESY spectra in D_2O solution. The strategies for sequence assignment of resonances in right-handed DNA and RNA helices have been extensively reviewed (Gronenborn & Clore, 1985; Patel et al., 1987; Hosur et al.,

Table II: Sequence Assignments of Some Nonexchangeable Protons of the Wheat Germ 5S rRNA Common Arm Fragment[a]

residue	H8/H6	H5	H1′
G_{30}	7.138		5.051
G_{31}	8.089		5.923
A_{32}	7.190		5.419
U_{33}	7.387	5.286	5.327
C_{34}[b]	7.785	5.700	5.752
C_{35}[b]	8.200	5.686	5.396
A_{43}[b]	8.121		5.071
C_{44}	8.210	6.063	6.108
U_{45}	8.180	6.260	5.897
C_{46}	7.358	5.200	5.567
C_{47}	7.817	5.812	5.535
G_{48}	8.058		6.312
A_{49}	7.363		4.832

[a] The entries in the table are chemical shifts in parts per million. For doublets, the number shown is the midpoint of the doublet. [b] This residue is in the loop.

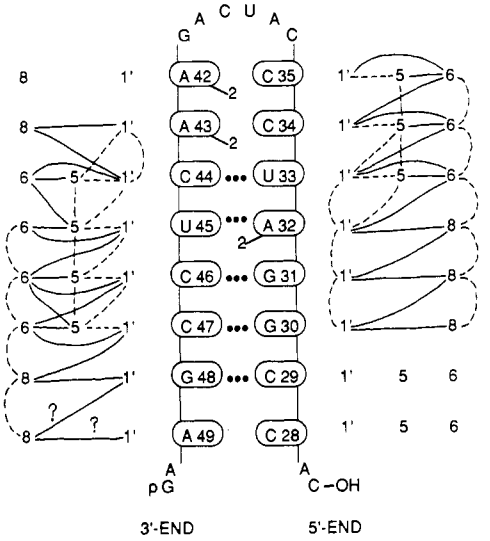

FIGURE 8: Schematic diagram showing observed NOESY connectivities between nonexchangeable protons of the wheat germ 5S rRNA common arm fragment, constructed from a base-paired model for the B2 fragment. The numbers on each side are the protons for each nucleotide. The dashed lines are connectivities for $(H8/H6)_n$–$(H8/H6)_{n+1}$ and $(H5/H1')_n$–$(H5/H1')_{n+1}$ pathways. The solid line is the $(H8/H6)_n$–$(H1')_n$–$(H8/H6)_{n+1}$–$(H1')_{n+1}$ pathway. Numbering system: 8 = H8; 6 = H6; 5 = H5; 2 = H2; 1′ = H1′. The question marks are connectivities identified from cross peaks of low signal-to-noise ratio.

1988; Van de Ven & Hilbers, 1988) and will not be repeated here. The three chemical shift ranges suitable for NOESY analysis are shown in Figures 5–7.

Figure 5 shows the $(H6/H8)_n$–$(H6/H8)_{n+1}$ (henceforth denoted the "d1 pathway") region of a NOESY spectrum acquired with a mixing time of 0.8 s. Figure 6 shows the $(H5/H1')_n$–$(H5/H1')_{n+1}$ ("d2 pathway") region of the same NOESY spectrum, which complements the information from Figure 5. The long mixing time was required to allow for development of significant NOE cross peaks in these two regions. The off-diagonal region, $(H6/H8)_n$–$H1'_n$–$(H6/H8)_{n+1}$–$H1'_{n+1}$ ("d3 pathway") shown in Figure 7 is the region normally used for resonance sequence assignment. That spectrum was obtained with a mixing time of 0.4 s to reduce spin-diffusion effects.

H5 and H6 are easily identified, since they give strong cross peaks at the same positions in Figure 7 as in the COSY experiment (see Figure 2 and Table I). The DQF-COSY experiment also identifies H1′ doublets (Figure 4 and Table I) by distinguishing them from other H1′ singlets. Except for a few unexpected extra connectivities (see below), sequence assignment is straightforward from Figures 5–7. Some observed and assigned NOESY connectivities are summarized in Figure 8, with their chemical shift values listed in Table II.

It is worth noting that several other short NOESY connectivities can also be established from Figures 5–7, but further assignments are precluded by multiple overlaps among those resonances. For example, the usually helpful assignment from $(H6/H8)_n$–$H2'_n$–$(H6/H8)_{n+1}$–$H2'_{n+1}$ or $(H6/H8)_n$–$H3'_n$–$(H6/H8)_{n+1}$–$H3'_{n+1}$ pathways in DNA cannot be used here because of resonance overlap: neither H2′ nor H3′ can be identified, except for the few H2′ which appear in DQF-COSY. In the NOESY assignments, the connectivities between the C_{33} H1′ and C_{33} H5 and between C_{34} H5 and C_{35} H5 are tentative because of the near-degenerate chemical shifts for members of each pair. In addition, the connectivities from G_{48} H1′ to A_{49} H8 to A_{49} H1′ ("?" in Figure 8) give only weak cross peaks.

Sequence-Specific Conformational Features. From Figure 8, we see that most of the NOESY connectivities are of the A-helix type. Moreover, if we include the C_{44}·U_{33} base pair as part of the helix, then the connectivities extend to the loop bases C_{34}, C_{35}, A_{43}, and probably to A_{49} at the other end of the helix. Similar base stacking extending into DNA hairpin loops is widely reported (Haasnoot et al., 1986, 1987; Blommers et al., 1987). In addition, the following sequence-specific conformational features of the B2 fragment are observed. First, all of the expected NOESY connectivities arising from the sequence from C_{28} to C_{35} are observed, except those from C_{29} to G_{30}. We conclude that most of this segment closely follows a typical RNA A-helix conformation.

However, in the sequence from A_{42} to A_{49}, four expected connectivities are missing: A_{43} H8 to C_{44} H6 to U_{45} H6; A_{43} H1′ to C_{44} H6; and C_{44} H1′ to U_{45} H6. Furthermore, three unexpected connectivities appear: A_{43} H8 to C_{44} H1′; C_{44} H6 to U_{45} H5; and C_{46} H6 to C_{47} H5. All but the last of these absent or extra connectivities occur between A_{43} and U_{45}, where C_{44} is proposed to form the unusual C_{44}·U_{33} base pair at the loop–helix junction. These NOESY anomalies evidently reflect the structural disruption (from an A-helix) occasioned by the unusual C·U pair. In support of this view, recall that C_{44} H1′ is the only assigned H1′ doublet (of 5) that could be identified by DQF-COSY: the C_{44} ribose is in a C2′-endo conformation, which produces an extension betwen residues A_{43} and C_{44} and a bend/turn between C_{44} and U_{45} (Jack et al., 1976). We suggest that ribose 44 adopts the C2′-endo conformation to allow the nucleotide to move inward from its neighbors to form the C·U pair, while at the same time preserving its connection to A_{43}. This compact (tight) loop–helix junction is consistent with independent NMR data from the exchangeable protons (Wu & Marshall, 1990). Finally, preliminary computer modeling and energy minimization results (Wu and Marshall, unpublished results) on the B2 fragment indicate that when distance constraints are applied to the C_{44}·U_{33} pair and other parts of the fragment are held in an A-helix conformation, the C·U pair is severely buckled, in accordance with the similar observation of DNA base pairs at hairpin loop–helix junctions (Haasnoot et al., 1987).

Maximum stability for an RNA helical stem closed by a hairpin loop is purportedly achieved when the loop comprises six or seven nucleotide residues, with five or six base extension of base stacking on the 5′-side of the helical stem and the remaining gap spanned by one or two nucleotides (Haasnoot et al., 1985; Blommers et al., 1987). In accord with this

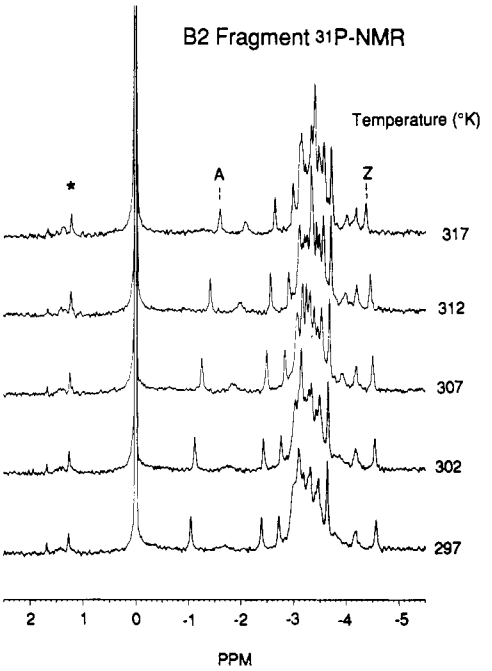

FIGURE 9: Heat-induced changes in a 121-MHz ^{31}P NMR spectrum of the wheat germ 5S rRNA common arm fragment in 10 mM sodium phosphate, pH 7.0, 99.996% D_2O solution. Two well-resolved resonances are labeled as A and Z. The resonance marked with a star is a degradation product.

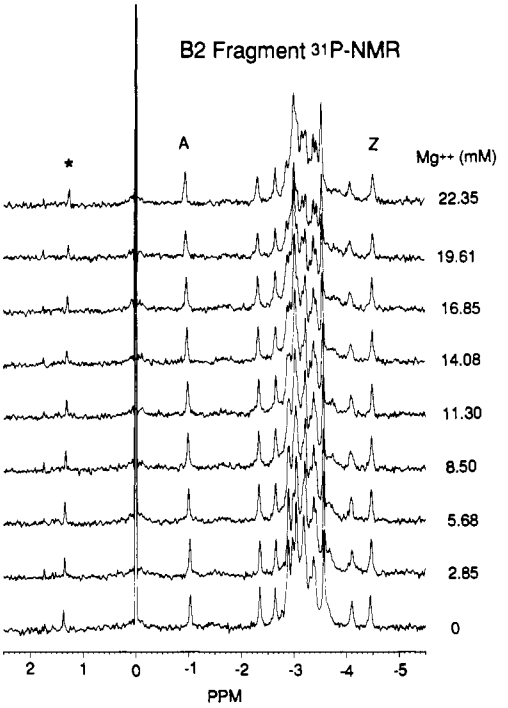

FIGURE 10: Mg^{2+} titration of a 121-MHz ^{31}P NMR spectrum of the wheat germ 5S rRNA common arm fragment in 10 mM sodium phosphate, pH 7.0, 99.996% D_2O solution. Resonances are labeled as in Figure 9.

principle, the present B2 fragment exhibits base stacking beyond the helix region. However, the base stacking extends only one nucleotide beyond the base-paired helix, and from the 3′-end rather than the 5′-end, on the basis of the observed NOESY connectivities. Perhaps the loop folding principle for RNAs is less general than has previously been supposed.

Temperature Variation and Mg^{2+} Titration Monitored by ^{31}P NMR Spectroscopy. The above proton NMR experiments mainly reflect the immediate environments of the base and H1′ (ribose) protons, which provide little information about the RNA phosphodiester backbone. Environmental perturbations such as heat or addition of Mg^{2+} produce marked changes in the NMR spectrum of the solvent-exchangeable protons of the B2 fragment (Wu & Marshall, 1990). We therefore next consider the effects of heat and Mg^{2+} on the ^{31}P NMR spectrum of the B2 fragment as a means of monitoring the RNA phosphodiester backbone conformation.

^{31}P NMR chemical shifts in phosphoesters are particularly sensitive to the O–P–O bond angle and P–O ester torsion angle, and ^{31}P NMR has been applied extensively to tRNAs [see review by Gorenstein (1984)]. For example, ^{31}P chemical shifts from a phosphate diester in a gauche, gauche (g, g) conformation are generally a few parts per million upfield from those of the more extended gauche, trans (g, t) or trans, trans (t, t) conformations. Moreover, a reduction in the O–P–O bond angle accompanies a change from a gauche to a non-gauche or trans conformation (and thus produces a downfield shift).

Figure 9 shows the temperature variation of the ^{31}P NMR spectrum of the B2 fragment. The low-abundance resonances between 1 and 2 ppm are degradation products, which increase in magnitude (not shown) on lengthy storage of the sample. The most prominent peak is inorganic phosphate, which is the buffer component and also serves as a convenient chemical shift reference. At 297 K, most of the ^{31}P resonances cluster near −3 ppm, representing the RNA backbone phosphodiesters that are primarily in native (g, g) conformations. At least 14 resonances can be partially resolved, indicating a range in individual phosphorus environments along the backbone. Two well-resolved resonances (A and Z, both assigned to have unit area) are seen on either side of the main group of resonances. Following the general principle stated above, peak A (~2 ppm downfield of the main group) probably exhibits a t, g conformation and may be located at a loop turning point. Similarly, peak Z (1–1.5 ppm upfield of the main cluster) represents a phosphorus with a greater degree of helix twist.

On increase in temperature, resonances in the main cluster shift slightly upfield and are somewhat better resolved. Peak A shifts upfield by ~0.55 ppm when heated from 297 to 317 K, corresponding to a winding of the (undertwisted) loop. Over the same temperature range, peak Z shifts downfield (by ~0.13 ppm) due to unwinding of the overtwisted part of the phosphodiester backbone. Thus, as temperature increases, all of the phosphate ester linkages move toward a common conformation of average helical twist: the loop segment twists tighter, and the helical segment unwinds somewhat. These results are consistent with those from temperature variation of exchangeable proton spectra of the wheat germ B2 fragment (Wu & Marshall, 1990) and from ^{31}P NMR results from yeast 5S rRNA (Burkey & Marshall, 1989).

Mg^{2+} titration of RNA spectra (both ^{1}H and ^{31}P NMR) has been widely used either as a tool of resonance assignment or to induce and monitor conformational changes (Marshall & Wu, 1989; Gorenstein, 1984). Specifically, binding of Mg^{2+} to the B2 fragment produces significant resonance shifts in the solvent-exchangeable ^{1}H NMR spectra in H_2O solution, explained as Mg^{2+}-induced stabilization of the RNA helix (Wu & Marshall, 1990). The results of Mg^{2+} titration of the B2 fragment on its ^{31}P NMR spectrum (Figure 10) support this conclusion. As the concentration of Mg^{2+} increases, peak A shifts downfield (by up to ~0.1 ppm), indicating a slight unwinding of that part of the loop, whereas peak Z shifts upfield (by up to ~0.06 ppm), indicating an increased helix twist at that phosphate. It should be noted that at this range of Mg^{2+} concentration the changes in the ^{31}P NMR spectrum

are relatively less pronounced than the corresponding changes in the ^1H NMR spectrum. Thus, Mg^{2+} binding is better monitored by ^1H NMR than ^{31}P NMR.

ACKNOWLEDGMENTS

We thank C. E. Cottrell for his expert advice in setting up the NMR experiments. We also thank our research group members J. E. Meier, J.-H. Kim, and H.-W. Huang for helpful discussions. The generous donation of wheat germ by International Multifoods (Columbus, OH) is gratefully acknowledged.

REFERENCES

Blommers, M. J. J., Haasnoot, C. A. G., Hilbers, C. W., Van Boom, J. H., & Van der Marel, G. A. (1987) in *Structure and Dynamics of Biopolymers* (Nicolini, C., Ed.) pp 78–91, Martinus Nijhoff Publishers, Dordrecht, The Netherlands.

Burkey, K., & Marshall, A. G., in Marshall, A. G., & Wu, J. (1989) *Biol. Magn. Reson.* (in press).

Chou, S.-H., Flynn, P., & Reid, B. (1989) *Biochemistry 28*, 2422–2435.

Clore, G. M., Gronenborn, A. M., & McLaughlin, L. W. (1985) *Eur. J. Biochem. 151*, 153–165.

Dobson, C. M., Olejniczak, E. T., Poulsen, F. M., & Ratcliffe, R. G. (1982) *J. Magn. Reson. 48*, 97–110.

Gronenborn, A. M., & Clore, G. M. (1985) *Prog. NMR Spectrosc. 17*, 1–32.

Gorenstein, D. G. (1984) in *Phosphorus-31 NMR, Principles and Applications* (Gorenstein, D. G., Ed.) pp 265–297, Academic Press, New York.

Haasnoot, C. A. G., & Hilbers, C. W. (1983) *Biopolymers 22*, 1259–1266.

Haasnoot, C. A. G., Den Hartoy, J. H. J., De Tooy, F. M., Van Boom, J. H., & Altona, C. (1980) *Nucleic Acids Res. 8*, 169–181.

Haasnoot, C. A. G., Hilbers, C. W., Van der Marel, G. A., Van Boom, J. H., Singh, U. C., Pattabiraman, N., & Kollman, P. A. (1986) in *Biomolecular Stereodynamics IV*, Proceedings of the Fourth Conversation in the Discipline Biomolecular Stereodynamics, SUNY at Albany, NY, June 4–9, 1985 (Sarma, R. H., & Sarma, M. H., Eds.) pp 101–115, Adenine Press, New York.

Haasnoot, C. A. G., Blommers, M. J. J., & Hilbers, C. W. (1987) in *Structure, Dynamics and Function of Biomolecules* (Ehrenberg, A., Rigler, R., Graslund, A., & Nilsson, L., Eds.) pp 212–216, Springer-Verlag, Berlin.

Happ, C. S., Happ, E., Nilges, M., Gronenborn, A. M., & Clore, G. M. (1988) *Biochemistry 27*, 1735–1743.

Hosur, R. V., Govil, G., & Miles, H. T. (1988) *Magn. Reson. Chem. 26*, 927–944.

Jack, A., Ladner, J. E., & Klug, A. (1976) *J. Mol. Biol. 108*, 619–649.

Lankhorst, P. P., Van der Marel, G. A., Wille, G., Van Boom, J. H., & Altona, C. (1985) *Nucleic Acids Res. 13*, 3317–3333.

Li, S.-J., & Marshall, A. G. (1985) *Biochemistry 24*, 4047–4052.

Li, S.-J., & Marshall, A. G. (1986) *Biochemistry 25*, 3673–3682.

Li, S.-J., Wu, J., & Marshall, A. G. (1987) *Biochemistry 26*, 1578–1585.

Luehrsen, K. R., & Fox, G. E. (1981) *Proc. Natl. Acad. Sci. U.S.A. 78*, 2150–2154.

Marion, D., & Wüthrich, K. (1983) *Biochem. Biophys. Res. Commun. 113*, 967–974.

Marshall, A. G., & Wu, J. (1990) *Biol. Magn. Reson. 9*, 55–118.

Patel, D. J., Shapiro, L., & Hare, D. (1987) *Q. Rev. Biophys. 20*, 35–112.

Redfield, A. G., & Kunz, S. D. (1975) *J. Magn. Reson. 19*, 150–254.

Van den Hoogen, Y. T., Erkelens, C., De Vroom, E., Van der Marel, G. A., Van Boom, J. H., & Altona, C. (1988) *Eur. J. Biochem. 173*, 295–303.

Van de Ven, F. J. M., & Hilbers, C. W. (1988) *Eur. J. Biochem. 178*, 1–38.

Wu, J., & Marshall, A. G. (1990) *Biochemistry* (preceding paper in this issue).

Wüthrich, K. (1986) *NMR of Proteins and Nucleic Acids*, Wiley, New York.